

Dear Jack (Associate Editor Jack Middelburg),

Thank you for your positive response to our BGD submission. As requested, we have detailed all relevant changes that we have made to the manuscript below. The changes closely follow those we proposed in our on-line response to the two Referees with one exception: we did not include the application of the open-water method (Odum, 1956) that we suggested in response to one of Referee #1's comments. Our rationale for not including this is given below.

All original comments from the Referees are written with 'Italic' font. How we have changed the texts is described with 'normal' font.

Changes made based on comments from Anonymous Referee #1:

This manuscript describes an important methodological advance for aquatic sciences by demonstrating that the eddy covariance method can be applied from the water-side of the air-water interface to measure oxygen and heat fluxes and to derive standard gas exchange coefficients. The method is used successfully at three shallow river sites where physical processes, especially heat exchange, are found to drive diurnal variations in gas exchange. The paper is well organized with careful, highly reasoned arguments for the approach and data treatments. The data examples are clear and mostly convincing.

We thank the Referee for the positive and constructive overall evaluation.

The only troubling part of the paper is sections that describe the possible methodological bias produced by temperature effects on the O₂ sensor time series and how the authors have corrected their measurements for this bias. Although I agree this bias is likely and needs to be understood, I do not think the authors have shown they really know its magnitude. They estimate a ~3% change in the oxygen reading per 1 degree C, and even with relatively small temperature fluctuations (<0.1 °C) this creates a bias about 3 times the measured signal (Figure 6). What if the effect was 4% or 2% instead of 3%? How consistent is the effect between optode sensors and their films? Is the effect proportional to the oxygen concentration or independent of oxygen concentration? Since the response time of the thermistor is faster than the optode, does this alter the correction? In short, the authors need to independently measure the magnitude of the temperature effect before applying a correction. This might be done with experiments where the oxygen partial pressure is held constant but temperature varied. Otherwise, the applied corrections may be creating more bias than they are removing.

Temperature effects or biases were an unexpected ancillary finding – the main focus was on quantifying air-water gas exchange by aquatic eddy covariance – but we can see that some

important details were missing, or not explained adequately. The following points were raised by the referee:

- 1) *They estimate a ~3% change in the O₂ reading per 1°C.* – This is not an estimate, it is a calculation based on the signal conversion equations given by the dual O₂-temperature sensor’s manufacture (JFE Advantech). According to the sensor manual we have (using manufacture’s nomenclature):

$$P' = \frac{A}{1 + D(t - 25) + F(t - 25)^2} + \frac{B}{N\{1 + D(t - 25) + F(t - 25)^2\} + C}$$

$$P = G + H \times P'$$

where $A, B, C, D, F, G,$ and H are fitting constants determined by the manufacture, t is the temperature [°C], N is the instrument output for O₂ [0 – 5 Volt], and P is the dissolved O₂ concentration [%]. By varying t for fixed values of N , the sensor’s temperature coefficient (% change in O₂ concentration reading caused by a temperature change of 1 °C) was calculated to range between 2.7 – 3.4%.

We did the lab experiments suggested by the Referee and measured a temperature coefficient of 2.9. We have added this extra information in Section 3.3 describing temperature effects.

- 2) *What if the effect was 4% or 2% instead of 3%?* – Assuming that the temperature fluctuations are the same, the temperature bias (false flux) is proportional with the temperature coefficient. We have added this information as well.
- 3) *How consistent is the effect between optode sensors and their films?* – Because the coefficients $A, B, C, D, F, G,$ and H only change a small amount, if at all (< 0 – 10%), from sensor to sensor and from film to film, we conclude that the effect is well-described by the information we have added as outlined above. We have chosen not to add these very specific details.
- 4) *Is the effect proportional to the O₂ concentration or independent of O₂ concentration?* – From the definition of the temperature coefficient (% change in O₂ concentration reading caused by a temperature change of 1 °C), the effect is proportional to the O₂ concentration. We have added this information.
- 5) *Since the response time of the thermistor is faster than the optode, does this alter the correction?* – The response time curves presented in Berg et al. (2016) were determined separately for temperature and for O₂. In additional lab tests we inserted

the dual O₂-temperature sensor from air into a water bath with both a significantly different temperature and O₂ concentration than the air. Since the response time curves looked similar to the ones shown in Berg et al. (2016), we assess that the minor difference in response times for temperature (0.34 s) and O₂ (0.51 s) does not affect the flux calculation or amplify the temperature bias. We have added this information.

If the authors can address the above concern any remaining revisions to the paper will be minor. Below are listed areas by line number that might be clarified.

Line 25. I question whether it is known that physical controls are “prevalent in lotic systems”. Perhaps it would be better to say “can be prevalent in lotic systems and adds uncertainty to assessments of biological activity for such systems that are based on water column O₂ concentration changes”.

We have changed the sentence to: “This physical control of gas exchange can be prevalent in lotic systems and adds uncertainty to assessments of biological activity that are based on measured water column O₂ concentration changes”.

Line 30. What is meant by “erosion in the surface water”? Erosion of what?

We have clarify this by changing the sentence to: “This was presumably caused by the formation and erosion of vertical temperature-density gradients in the surface water driven by the heat flux into or out of the river that affected the turbulent mixing”.

Lines 78-80. Awkward sentence. Please restructure.

We have changed the sentence to: “Turbulence, or turbulent-like motion, that affects or controls the thickness of the film on the water side, and thus the diffusive resistance to gas transport, can be driven by conditions both below and above the air-water interface”.

Line 87. Omit “but” in this sentence.

We have done so.

Line 93. Indicate where and how the tracer additions are made.

We have clarified this by changing the sentence to: “For smaller rivers and streams they include targeted parallel up-and across-stream additions of volatile tracers (e.g. propane) and hydrologic tracers (e.g. dissolved chloride), where the latter is added to correct for

dilution of propane due to hyporheic mixing (Genereux and Hemond 1992; Koopmans and Berg 2015)“.

Lines 103-104. Change “studied” to “studies” and then clarify what is meant by “fitting measurements done in other aquatic systems”.

We have corrected the typo and addressed this question by changing the sentence to: “Partly motivated by the substantial and often methodologically challenging effort required to measure k at specific sites with any of these approaches, many studies have simply relied on general empirical correlations for k produced by fitting k values measured for other similar aquatic systems (Raymond and Cole 2001; Borges et al. 2004; Cole et al. 2010)”.

Line 108. “many standard estimates” of what? Please clarify. Are you talking about carbon budgets?

We have added: “...such as gross primary production, respiration, and net ecosystem metabolism”.

Line 125. Rerword as: “we were able to derive parallel fluxes. . .”

We have done so.

Line 126. Rerword as: “proof-of-concept tests that were up to 40 hours long at three river sites.”

We have done so.

Line 131. Rerword as: “All measurements were made from. . .”

We have done so.

Line 140. How was the measurement position ~5 cm below the interface determined?

We have clarified this by changing the sentence to: “This type of ADV allowed the sensor head to be positioned facing upwards (Fig. 1) while recording the velocity field right below the air-water interface, typically ~4 cm. This distance was determined from standard ADV output”.

Later (line 222) can you indicate how sensitive the storage term correction is to changes in this measurement?

We have added this information in Section 3.1 where we present the O₂ fluxes shown in Fig. 2.

Line 144. Why is the sensor not identified as manufactured by Rinko?

We have added this information.

Line 155. Separate into two sentences here. Indicate how reproducible the response times are with each fresh sensor film put on the optode tip.

We have split the sentence in two. We have added this information in Section 2.1 where we first present the sensor's response times for O₂ concentration measurements.

Line 158. Why reference Fig. 2a here?

This was a mistake. We have corrected it to Fig. 1a.

Line 169. Change to "PAR sensor".

We have done so.

Line 183. "as level as possible" is vague. Can you indicate within a certain number of degrees from vertical? Please clarify how tilt changes were corrected for within the time span of a 15-min burst as the sensor must bob up and down some.

We have reworded the sentence to: "Using a level and by placing dive weights on the platform (Fig. 1b) care was taken to ensure that it was horizontal within the tolerance of the level to minimize post-processing rotations of the velocity field to correct for sensor tilt".

We don't think it is possible to specify a value for this tilt. However, for the deployment shown in Figs. 2 and 3, rotations to nullify the mean vertical and transverse velocity, resulted in an average rotation angle with horizontal of only 1.3 degrees, and did not affect the flux calculation. We added this information in Section 3.1 where this deployment is presented.

Also, as described in Section 2.2, all river sites used for our proof-of-concept tests were chosen to have "smooth and quietly flowing water without standing riffles or waves". As a result, our sensors did not bob up and down during measurements. Consequently, a correction for such complex sensor movements was deemed unnecessary. We added a sentence stating that in Section 2.2.

Line 191. The key word here is “detectable”. There may still be high frequency signals lost because they are not detectable by these sensors.

We agree, and note that we did use the word “detectable” here. We doubt though, that the “undetectable” part of the flux signal has any significant magnitude given the steep drop-off of the flux contribution at the high-frequency end of the co-spectrum (Fig. 4) combined with the sensors response time ($t_{90\%}$: 0.51 s for O₂ and 0.34 s for temperature). We mention this at the very end of section 3.1 and have not added a more detailed discussion of this complex question.

Line 227. It would be helpful here if the authors gave more information about how the “Spectra version 1.2” code treats the data. Also, what is meant by “several consecutive data segments”? How does this relate to what is shown in Fig. 4?

We have added the requested information so that the paragraph reads: “To examine the eddy frequencies that carried the flux signal, cumulative co-spectra of the O₂ concentration and the vertical velocity were calculated for representative periods in each deployment with minimally varying fluxes using the software package Spectra version 1.2 (P. Berg unpubl.). This software essentially performs the identical flux calculation in the frequency domain after fast Fourier transforming the de-trended data as EddyFlux does in the time domain. Both software packages rely on the same means of de-trending and time shifting data”.

Also, in the presentation of Fig. 4, the specific time interval behind the two co-spectra is mentioned specifically.

Line 237. It would be helpful for the authors to present the relationships for calculating k_{600} even though they are in the papers cited.

To do this in a meaningful way would add two equations and a separate paragraph to explain this calculation well. Since it is a standard conversion in the gas exchange literature we suggest that we do not add this. However, because the conversion is outlined best and most straight forward in the referenced Cole et al. 2010 paper, we have removed the two other papers cited.

Line 256. Since the data is presented as hourly fluxes, why not change the units in the figures to per hour rather than per day?

We prefer to use the unit mmol m⁻² day⁻¹, in part because this unit is often used for measures such as net ecosystem metabolism.

Line 269. Suggest reword as: “controlled by a driver apart from the river current velocity or winds. . .”.

We have done so.

Line 272. Unclear what results are being referred to here.

These are data from a stable independent dual O₂-temperature sensor. It is defined specifically in line 167, and we have added that we refer to this sensor as “the independent sensor” throughout the manuscript.

Line 317. I do not see why the authors reference Gundersen et al. 1998 here? This paper discusses the temperature sensitivity of oxygen microelectrodes that operate by different principles than optodes. The microelectrode temperature effect is usually related to the gas solubility in the membrane and changes in the diffusion rate.

This referenced paper does indeed focus on microelectrodes. It is the only reference we have been able to find that gives information on the temperature coefficient for any type of fast-responding O₂ sensor. It is relevant because microelectrodes that apparently suffer from the same temperature dependency as optical sensors are still by far the most common sensor type used for aquatic eddy covariance. However, we acknowledge that this was not explained well, and we have elaborated on this as suggested in our response to the Referee’s main comment (see above).

Lines 352-355. Good argument here. Correct the spelling of “concentration” in line 355.

We have corrected this.

Line 371. Reword as: “This, in turn, changed the. . .”

We have corrected this.

Line 380-383. Can the authors take this argument further perhaps with an illustrative example?

If we had a good measurement of the average water depth, or a way to assess it, we could apply the standard “open water” technique (Odum, 1956) and estimate the benthic flux for evaluation. However, without this information we think this exercise would become too speculative and uncertain, and thus, not serve as a meaningful example supporting our point.

Line 399. Do the authors have any temperature profiles from their sites that may illustrate temperature stratification during the day?

No, unfortunately not, but this is something we would like to add in future studies.

Line 410. Change to: “was first developed”

We have corrected this.

Lines 416-417. It is unsatisfying that the authors call for more studies of the temperature bias. As noted above, they need to include more concrete studies in the context of this paper.

In response to the Referee’s main comment, we have added more information along these lines (see above). However, the main focus of our manuscript is the new approach for determining air-water gas exchange rates and coefficients, whereas the temperature bias is an ancillary finding. Conversely, we find it acceptable to suggest that more work is needed along those lines.

Line 436-437. It would be helpful if earlier in the paper the authors indicated the magnitude of the O₂ storage term relative to Jeddy (Equation 3).

We have added this information in Section 3.1 where we present the O₂ fluxes shown in Fig. 2.

Table 1. Add standard deviations to the parameters in the right three columns.

We have reported SEs throughout the paper and can add these to Table 1.

Figure 1c. Add arrows to indicate each identified item and indicate that the “independent dual O₂-temperature sensors” are the miniDOT sensors and the sensor used for EC is a Rinko sensor.

We have added this information.

Changes made based on comments from Anonymous Referee #2:

The manuscript by Peter Berg and Michael Pace investigates air-water gas exchange at three shallow river sites. The authors focus on the determination of oxygen and temperature exchange by using the eddy covariance technique on a floating platform to assess gas exchange coefficients. The major findings show that oxygen dynamics (on an hourly scale) are largely independent of current velocities and biological activity; instead oxygen dynamics are driven

by heat exchange, i.e. changing oxygen saturations. Furthermore, the authors point out the importance of high resolution temperature measurements to correct for the oxygen sensor specific temperature sensitivity.

The manuscript is well written / structured and of interest for a broader readership as the results have important implications for the growing community that uses the aquatic eddy covariance technique. The approach to determine gas exchange coefficients using the temperature+oxygen eddy covariance technique is also a methodological advance.

We thank the Referee for the positive and constructive overall evaluation.

However, the manuscript is lacking some important details and it would benefit from a more in-depth analysis of the interesting and promising dataset. The heat-exchange driven oxygen fluxes are only masking the more interesting biogeochemical processes and are overemphasized. In the current version, the discussion about the temperature bias raises more questions than it actually resolves. See below for a detailed argumentation.

Argumentation:

1. One of the key findings and also a major part of the discussion is that heat exchange is driving most of the oxygen dynamics in shallow-water rivers. This is reasonable on timescales of hours, however, the physical process is only masking the biogeochemical processes which are still occurring and which are of importance. Based on the dataset it should be easily possible to distinguish between the biologically induced oxygen fluxes and the heat exchange induced oxygen fluxes. On the long run, the heat exchange induced fluxes should also average out implying a limited role for net exchange fluxes. When the authors follow my recommendation they could subtract the heat exchange induced oxygen flux from the total flux. I am convinced that this procedure will reveal good correlations with parameters like flow velocity and biological activity.

We agree that physical processes are “masking the biogeochemical processes which are still occurring and which are of importance”, but we do not understand how “it should be easily possible to distinguish between the biologically induced oxygen fluxes and the heat exchange induced oxygen fluxes”. We agree that this would be desirable, but we cannot see a way to split the total O₂ flux that we measured into these two components. It is suggested to “subtract the heat exchange induced oxygen flux from the total flux”, but how do we quantify the heat exchange induced O₂ flux? Maybe this suggestion is rooted in misreading Fig. 3 which shows the actual heat flux, and not the heat exchange induced O₂ flux?

2. *The effect of temperature fluctuations on the oxygen measurement is convincing but in the current version of the manuscript it raises several questions that need to be addressed:*

Referee #1 echoed this point too, stating that important details on the effect of temperature fluctuations were missing, or not explained adequately. Please see our response to Referee #1 and the additional information below.

Resolution: The authors are discussing the response time of the temperature sensor, which is indeed in the range of the oxygen sensor. However, the sensor tip is much thicker (8mm, line 154) which implies that the spatial resolution is limiting the minimum eddy size, i.e. frequency, that can be resolved.

The diameters of the thermistor and the active O₂ sensing foil are ~1 mm and ~5 mm, respectively, and the thermistor is positioned ~2 mm away from the edge of the foil. These dimensions should be considered in relation to the measuring volume of the Acoustic Doppler Velocimeter (ADV) which has a 14 mm diameter and is 14 mm tall. In that light, the limiting factor of what eddy sizes, or frequencies, can be resolved is associated with the ADV and not the dual O₂-temperature sensor. We have explained this point in Section 2.1 where we describe our sensors.

Sampling Rate / Correction Procedure: The “real” sampling rate of the oxygen sensor and temperature sensor differ as the response times are slightly different and there is also a distance between the two sensors. How did the authors ensure that the temperature measured is similar to the one at the oxygen sensor tip? Did the authors also apply a time shift correction?

The response times reported in Berg et al. (2016) are 0.34 s for temperature and 0.51 s for O₂. Because of that, and because of the slightly different distances from the thermistor and O₂ sensing foil to the center of the ADV's measuring volume, we applied independent time shift corrections for the heat flux and the O₂ flux. We did originally explain how the time shift was performed for O₂, and we have added that this correction was applied independently for the heat flux.

Range of Error: The example depicted in Figure 6 indicates that in the case of systems with large heat exchange, basically all measurements without temperature-correction are wrong. Therefore, this kind of correction needs a careful assessment. It would be interesting to see the temperature correction applied in Figure 2 for the hourly oxygen fluxes.

The text was unclear about this, but the temperature correction was applied to the O₂ fluxes shown in Fig. 2, as it was to all data we report. It is only for one data example shown in Fig. 6 that this correction was not applied to illustrate the severe effect that omitting the

temperature correction can have. We have stated this clearly in Section 2.3 where we describe our flux calculation protocol and also in the Fig. 6 legend.

Figure / table / line specific comments:

Figure 5: It is of interest to present the missing correlation between the gas exchange coefficient and flow velocity, however this should be contrasted by an existing correlation. An example could be the comparison of the temperature gradient versus the gas exchange coefficient. This correlation would strengthen the argumentation.

We do not understand the first suggestion here. With respect to showing the gas exchange coefficient vs. the temperature gradient (the vertical one?), unfortunately we do not have any temperature measurements down through the top of the water column, but this would indeed be an interesting analysis to make in future studies.

Table 1: Most of the oxygen flux is driven by heat exchange, which shows most of its variation on a daily basis. The presented oxygen fluxes are averaged in time intervals of 1 hour – 12 hours and are, therefore, strongly biased. As a result the variability within the oxygen fluxes is arbitrary as it only depends on the cut-off time.

We disagree that our tabulated O₂ fluxes are “strongly biased” and that their variability is “arbitrary” and “only depends on the cut-off time”. In Section 3.2 we stated specifically that the fluxes in Table 1 and the derived gas exchange coefficients represent periods of time with several successive 15-min time intervals that had little variation and appeared to represent a particular field condition. We don’t know how to address this point any better.

Line 103: many studies.

We have fixed this typo.

Line 135: It is not very convincing that a floating platform is stable when fixed as described. Actually, I would expect movements that are in the range of the eddies that carry the oxygen signal.

As we state in Section 2.2, all sites were picked because they had smooth and quietly flowing water without standing ripples or waves. We regard our tests as proof-of-concept deployments and aimed carefully at keeping the field conditions as simple as possible. We didn’t observe any vertical movements of the platform or even eddies distorting the air-water interface. Although less critical for the flux calculation, we did not observe any lateral

movements of the platform either due to the two-point anchoring system we used. We have expanded the explanation of this in Section 2.2.

Line 185 and 196: How accurate was the positioning / how big was the sensor tilt? It is not clear if the correction for the sensor tilt was performed or not.

It is difficult to put a number on this sensor tilt, but for the deployment featured in Figs. 2 and 3, the average rotation with horizontal direction to nullify the mean vertical and transverse velocity was only 1.3 degrees and did not affect the flux calculation. We have added this information in Section 3.1 where we present this deployment.

Line 210: It should be stated in which range the time shift is. Considering the very constant flow velocity and the known response times it should be possible to calculate it. The time shift should not be bigger than the time it needs to travel from the ADV measuring volume to the sensor tip + response time!?

Due to a micro boundary layer forming on the O₂ sensing foil, the actual time shift found as described in Section 2.3 is slightly larger than suggested by the Referee. Again, for the deployment in Fig. 2, the averaged time shift equaled 1.3 s. We have added this information in Section 3.1 where we present this deployment.

Line 219: Equation 3 is not adequately described, what does the second term imply, how is it measured, what is the range relative to the eddy covariance flux.

We agree, Eq. 3 was not adequately explained. We have corrected this and also provided an average number for the magnitude of the storage relative to the eddy flux as suggest by Referee #1.

Line 239: To my knowledge “lumped” is not a statistical method.

Please note that we do not claim that. We find that the description of how to generate 8 Hz data from 64 Hz data is sufficient.

Continuous measurement of air-water gas exchange by underwater eddy covariance

Peter Berg, Michael. L. Pace

5

Department of Environmental Sciences, University of Virginia, Charlottesville, Virginia, USA

Correspondence to: Peter Berg (pb8n@virginia.edu)

10 **Abstract.** Exchange of gasses, such as O₂, CO₂, and CH₄, over the air-water interface is an important component in aquatic ecosystem studies, but exchange rates are typically measured or estimated with substantial uncertainties. This diminishes the precision of common ecosystem assessments associated with gas exchanges such as primary production, respiration, and greenhouse gas emission. Here, we used the aquatic eddy covariance technique – originally
15 developed for benthic O₂ flux measurements – right below the air-water interface (~5-4 cm) to determine gas exchange rates and coefficients. Using an Acoustic Doppler Velocimeter and a fast-responding dual O₂-temperature sensor mounted on a floating platform the 3D water velocity, O₂ concentration, and temperature ~~are-were~~ measured at high-speed (64 Hz). By combining these data, concurrent vertical fluxes of O₂ and heat across the air-water interface ~~are-were~~ derived, and
20 from the former, gas exchange coefficients. Proof-of-concept deployments at different river sites gave standard gas exchange coefficients (k_{600}) in the range of published values. A 40 h long deployment revealed a distinct diurnal pattern in air-water exchange of O₂ that was controlled largely by physical processes (e.g., diurnal variations in air temperature and associated air-water heat fluxes) and not by biological activity (primary production and respiration). This physical control of gas exchange ~~is prevalent in lotic systems and adds uncertainty to common ecosystem assessments of biological activity relying on water column O₂ concentration recordings~~ can be

25

prevalent in lotic systems and adds uncertainty to assessments of biological activity that are based on measured water column O₂ concentration changes. For example, in the 40 h deployment, there was close-to constant river flow and insignificant winds – two main drivers of lotic gas exchange – but we found gas exchange coefficients that varied by several fold. This was presumably caused by the formation and erosion of vertical temperature-density gradients ~~formation and erosion~~ in the surface water driven by the heat flux into or out of the river that ~~controlled~~ affected the turbulent mixing. This effect is unaccounted for in widely used empirical correlations for gas exchange coefficients and is another source of uncertainty in gas exchange estimates. The aquatic eddy covariance technique allows studies of air-water gas exchange processes and their controls at an unparalleled level of detail. A finding related to the new approach is that heat fluxes at the air-water interface can, contrary to those typically found in the benthic environment, be substantial and require correction of O₂ sensor readings using high-speed parallel temperature measurements. Fast-responding O₂ sensors are inherently sensitive to temperature changes, and if this correction is omitted, temperature fluctuations associated with the turbulent heat flux will mistakenly be recorded as O₂ fluctuations and bias the O₂ eddy flux calculation.

1 Introduction

1.1 Background

Exchange rates of gasses over the air-water interface in rivers, streams, reservoirs, lakes, and estuaries are key parameters for estimating a number of important ecosystem variables (Cole et al. 2010). Gas exchange rates are used to estimate metabolism of aquatic systems (Hanson et al. 2004; Van de Bogert et al. 2007; Van de Bogert et al. 2012), emission of greenhouse gasses like CO₂ and CH₄ to the atmosphere (Cole et al. 2010), and the role of inland and near-shore waters in regional (Billett and Moore 2008) and global (Cole et al. 2007; Bastviken et al. 2011) carbon cycling. As a result, over several decades a tremendous effort among aquatic scientists has focused on understanding and quantifying gas exchange processes at the air-water interface and

55 their controls under naturally occurring field conditions (Whitman 1923; Butman and Raymond
2011; Raymond et al. 2013).

Multiple state variables and complex physical processes on both sides of the air-water interface
control gas exchange (Macintyre et al. 1995; MacIntyre et al. 2010). Despite this complexity, the
60 widely used expression for gas exchange rates was formulated based on a conceptually simple
model assuming that gas is transported by molecular diffusion across intact boundary layers, or
thin films, found on each side of the interface (Whitman 1923; Liss and Slater 1974):

$$J_{air-water} = k(C_{water} - C_{air}) \quad (1)$$

65 where $J_{air-water}$ is the exchange rate, or vertical flux, of the gas (positive upward), C_{water} is the gas
bulk concentration below the film on the water-side, C_{air} is the concentration above the film on the
air-side, and k is the gas exchange coefficient, often also referred to as the ‘gas transfer velocity’ or
‘piston velocity’. For most gasses, C_{water} and C_{air} are straight forward to measure with modern
70 sensors (Koopmans and Berg 2015; Fritzsche et al. 2017), or calculate from known functions, but
the complexity of gas exchange and its many controlling variables is contained in k (Macintyre et
al. 1995; McKenna and McGillis 2004; Cole et al. 2010).

For sparingly soluble gasses such as O_2 , CO_2 , and CH_4 , the ratio between the molecular diffusivity
75 in air and water is on the order of 10^4 . Consequently, the resistance to gas diffusion is associated
with the film on the water-side, even if a substantially thicker film is found on the air-side of the
air-water interface. This means that in the case of O_2 , C_{air} is simply the saturation concentration of
 O_2 in water, which is a well-described function of the water temperature and salinity (Garcia and
Gordon 1992) and the atmospheric pressure.

80 Turbulence, or turbulent-like motions, that affects or controls the thickness of the film on the
water side, and thus the diffusive resistance to gas transport, can ~~originate from~~ be driven by

conditions both below and above the air-water interface. In shallow streams and rivers, this turbulence is typically generated by the water flow over an uneven or rough bottom. Substantial heat loss from the water can similarly result in density driven water motion that erodes the film (Bannerjee and MacIntyre 2004). On the contrary, in reservoirs, lakes, and estuaries, the turbulence on the water side of the interface is typically generated by wind, which makes wind speed the dominant controlling variable for k for such systems (Marino and Howarth 1993). Despite the fact that typical conditions such as rough weather, surface waves, and rain can rupture the films on the water side, the simple expression for gas exchange (Eq. 1) is still applied, ~~but~~ with k values that are adjusted accordingly (Watson et al. 1991). Keeping these multivariable, highly dynamic, and complex controls in mind, it is evident that determination of representative k values for specific sites is a challenging task.

1.2 Formulation of problem

A number of approaches have been used to study and determine values for k . For smaller rivers and streams they include targeted parallel up-and across-stream additions of volatile tracers ~~such as (e.g. propane)~~ and hydrologic tracers ~~such as (e.g. dissolved chloride)~~, where the latter is added to correct for dilution of propane due to hyporheic mixing (Genereux and Hemond 1992; Koopmans and Berg 2015). A common approach for smaller reservoirs and lakes relies on additions of inert tracers, e.g. SF₆ (Wanninkhof 1985; Cole et al. 2010), whereas floating chambers are often deployed in larger rivers, reservoirs, lakes, and estuaries (Marino and Howarth 1993). In a limited number of studies of large reservoirs and lakes, tower-mounted atmospheric eddy covariance systems have been used to measure air-water exchange, and from that, k values were derived (Anderson et al. 1999; Jonsson et al. 2008; Mammarella et al. 2015). Partly motivated by the substantial and often methodologically challenging effort required to measure k at specific sites with any of these approaches, many studied studies have simply relied on general empirical correlations for k produced by fitting measurements done in k values measured for other similar aquatic systems (Raymond and Cole 2001; Borges et al. 2004; Cole et al. 2010). With the exception of atmospheric eddy covariance measurements, none of these approaches represent a

direct way of determining k values because they rely on assumptions that often are difficult to assess, or simply not fulfilled. As a result, gas exchange is viewed among aquatic scientists as the primary source of uncertainty in many standard estimates for aquatic systems such as gross primary production, respiration, and net ecosystem metabolism (Wanninkhof et al. 1990; Raymond and Cole 2001; Raymond et al. 2012).

1.3 Scope of work

The aquatic eddy covariance technique for O_2 flux measurements under undisturbed in situ conditions was originally developed for the benthic environment (Berg et al. 2003). The approach has several significant advantages over other flux methods, including its non-invasive nature (Lorrai et al. 2010), high temporal resolution (Rheuban & Berg 2013), and its ability to integrate over a large benthic surface (Berg et al. 2007). As a result, it has been used to measure whole-system fluxes for substrates such as river bottoms (Lorke et al. 2012; Berg et al. 2013), seagrass meadows (Hume et al. 2011; Rheuban et al. 2014), and coral reefs (Long et al. 2013; Rovelli et al. 2015).

Here, we applied the aquatic eddy covariance technique ‘upside down’ right below the air-water interface to measure O_2 fluxes. From them, we derived exchange coefficients for O_2 , and then standard gas exchange coefficients (k_{600}). All measurements were done from a floating platform, and because we used a newly developed fast-responding dual O_2 -temperature sensor (Berg et al. 2016), we ~~get~~ were able to derive parallel fluxes of O_2 and thermal energy, or sensible heat. We conducted proof-of-concept tests ~~including deployments at three river sites that were up to 40 hours long that were up to 40 h long at three river sites.~~

2 Methods

2.1 Floating measurements platform

All measurements were ~~done~~ made from a 1.2 × 0.9 m floating platform with a catamaran-shaped hull (Fig. 1) that was kept at a fixed position at the river sites by two upstream anchors. ~~Due to this setup and the current's constant pull on the hull, the platform was stationary during deployment.~~ The modular design and the catamaran-shaped hull allow the platform to be collapsed for storage and easy shipment in a standard sturdy Polymer ~~gun~~ case (Pelican Products, USA).

The 3D velocity field was measured with an Acoustic Doppler Velocimeter (ADV) with a cabled sensor head (cabled Vector, Nortek AS, Norway). This type of ADV allowed the sensor head to be positioned facing upwards (Fig. 1) while recording the velocity field right below the air-water interface ~~(typically ~5 cm), typically ~4 cm. This distance was determined from standard ADV output.~~ Data were collected continuously at a rate of 64 Hz and represent water velocity values averaged over the ADV's cylindrical measuring volume (h ~1.4 cm, Ø ~1.4 cm) located 15.7 cm above the sensor head (Fig. 1).

The O₂ concentration was measured with a new fast-responding dual O₂-temperature sensor (RINKO EC, JFE Advantech, Japan) developed specifically for eddy covariance measurements (Berg et al. 2016). ~~which, combined with the velocity data, This sensor~~ allows for simultaneous fluxes of O₂ and ~~sensible~~ heat to be derived. ~~and also It also allows~~ instantaneous temperature correction of the O₂ concentration. signal. This sensor was developed specifically for eddy covariance measurements (Berg et al. 2016) and The sensor was designed to interface with our standard ADVs (Vectors, Nortek AS, Norway) through a single cable supplying power to the sensor and also transmitting its two outputs, one for O₂ and one for temperature, to the ADV's data logger to be recorded along with velocities to ensure perfect time alignment of all data. The O₂ measuring part of this new sensor is a small 6 mm diameter planar optode and concentrations are determined from fluorescence life-time measurements (Klimant et al. 1995; Holst et al. 1997; Holst et al. 1998). The tip of the sensor tip size, including which contains both the temperature thermistor and the O₂ sensing foil, has a diameter of 8.0 mm which makes it far more robust than

O₂ microsensors typically used for aquatic eddy covariance measurements. Yet because the sensor's tip is still only half the size of the ADV's measuring volume, it will not limit the eddy size that can be measured by the system. and itsThe sensor's response times ($t_{90\%}$) were measured to be 0.51 ± 0.01 s (SE, n = 7) for O₂ and 0.34 ± 0.01 s (SE, n = 9) for O₂-and-temperature, respectively (Berg et al. 2016). The same response time for O₂ was consistently found when the O₂ sensing foil was replaced (an easy user performed operation typically needed after ~10 days of continuous use). The edge of the sensor tip was positioned ~2.0 cm downstream of the edge of the ADV's measuring volume so that water passed through this volume before sweeping over the angled O₂ sensing tip (Fig. [2a1a](#)). This setup ensured undisturbed measurements of the natural current flow. Power was supplied from an external battery (Fig. 1a) with a capacity that allowed 64 Hz data to be collected continuously for at least 48 h. Because all instrument components were designed for underwater use they are not affected by rain or humid conditions.

Measurement of supporting environmental variables during each deployment allowed verification of recorded data and assisted in the interpretation of the derived eddy fluxes. These variables included mean O₂ concentration and temperature at the measuring depth recorded every 1 min with one or two stable independent dual O₂-temperature sensors (miniDOT, PME, USA, referred to as the independent sensor below). In some-most deployments photosynthetically active radiation (PAR) was ~~also~~ recorded at the measuring depth every 5 min using an independent submersible PAR sensors (Odyssey, Dataflow Systems, New Zealand). For one deployment, light data were taken from nearby meteorological weather stations.

2.2 Field tests

The new approach for determining air-water gas exchange rates and associated exchange coefficients from underwater eddy covariance measurements was tested at three river sites, all in Virginia (US), one in the Hardware River, one in the Mechums River, and one in Moormans River. All sites had a fairly linear run with a water depth between ~0.3 and ~1 m and smooth and quietly flowing water ([Fig. 1c](#))-without standing riffles or waves. As a result of this, the two-point

195 anchoring system, and the current's constant pull on the hull, the platform was stationary during
measurements. Typical surface flow velocities ranged from 6 to 30 cm s⁻¹. The ADV and the fast-
responding O₂-temperature sensor were adjusted to record data ~54 cm below the air-water
interface. Four deployments lasting up to 40 h were initiated on November 22, 2015 and
September 14, 2016 in the Hardware River and on December 21, 2016 and January 18, 2017 in
the Moormans River. Using a level and by placing dive weights on the platform (Fig. 1b) care was
200 taken to ensure that ~~the instrument was as level as possible~~ the platform was horizontal within
the tolerance of the level to minimize post-processing rotations of the velocity field to correct for
sensor tilt.

2.3 Calculations of eddy fluxes

205 Fluxes of O₂ ~~and heat~~ were extracted from the raw eddy covariance data following the ~~same~~-multi-
step process briefly described below ~~for O₂~~.

Using the two simultaneously measured outputs from the fast-responding dual O₂-temperature
sensor, one for O₂ and one for temperature, the O₂ concentration was calculated from the
210 calibration equation provided by the manufacture. Because this equation contains both outputs,
this calculation includes instantaneous temperature correction of the O₂ concentration evaluated
in detail below. If needed, the O₂ concentration was calibrated against the ~~stable~~-independent ~~dual~~
~~O₂-temperature~~ sensor data. All 64 Hz data were then reduced to 8 Hz data, which reduces noise
while providing sufficient resolution to contain the full frequency spectrum carrying the
215 detectable flux signal (Berg et al. 2009). This assumption was validated by comparing fluxes
calculated from both 8 and 64 Hz data for a subset of the data.

O₂ fluxes, one for each 15-min data segment, were extracted from the 8 Hz data using the software
package EddyFlux version 3.1 (P. Berg unpubl.). If needed, this software rotates the flow velocity
220 field for each data segment to correct for any sensor tilt (Lee et al. 2004; Lorrai et al. 2010; Lorke

et al. 2013) bringing the transverse and vertical mean velocities to zero. The vertical eddy flux was then calculated as (defined positive upward):

$$J_{eddy} = \overline{w'C'} \quad (2)$$

225

where the overbar symbolizes the averaging over the 15-min data segment, and w' and C' are the fluctuating vertical velocity and the fluctuating O₂ concentration, respectively. These fluctuating components are calculated as $w - \bar{w}$ and $C - \bar{C}$ where w and C are measured values (at 8 Hz), and \bar{w} and \bar{C} are mean values defined as least square linear fits to all w and C values within the 15-min time segment, a procedure usually referred to as linear de-trending (Lee et al. 2004; Berg et al. 2009).

230

Due to the response time of the dual O₂-temperature sensor and its position downstream from the ADV's measuring volume, a time shift correction was applied. This was done by repeating the outlined flux ~~extraction procedure calculation~~, while shifting the 8 Hz O₂ concentration data back in time, 1/8 s at a time, until the numerically largest flux was found.

235

Estimating the gas exchange coefficient requires the O₂ flux over the air-water interface to be known. However, the eddy flux, J_{eddy} (Eq. 2), is measured ~54 cm below the interface. By using the linear fit to the measured O₂ concentrations in each 15-min data segment, defined as \bar{C} above, J_{eddy} is corrected for storage of O₂ in the ~54 cm volume column of water to give the flux at the air-water interface:

240

$$J_{eddy, air-water} = J_{eddy} - \int_0^h \frac{d\bar{C}}{dt} dz \quad (3)$$

245

where h is the ~54 cm tall water column, and the integral represents the change in time of O₂ stored in this column. For further details on this flux extraction protocol included in EddyFlux

version 3.1, see Lorrai et al. (2010), Hume et al. (2011), and Rheuban et al. (2014). For presentation, the 15-min fluxes were lumped in groups of four to give hourly values.

250 To examine the eddy frequencies that carried the flux signal, cumulative co-spectra of the O₂ concentration and the vertical velocity were calculated for ~~several consecutive data segments representative periods in each deployment in each deployment, cumulative co-spectra of the O₂ concentration and the vertical velocity were calculated~~ using the software package Spectra version 1.2 (P. Berg unpubl.). This software essentially performs the identical flux calculation in the frequency domain after fast Fourier transforming the de-trended data as EddyFlux does in the time domain. Both software packages rely on the same methods for de-trending and time shifting data.

260 Heat fluxes and associated co-spectra were extracted from the raw eddy covariance data following the same multi-step process.

2.4 Calculations of gas exchange coefficients

265 The saturation concentration of O₂ (C_{air} in Eq. 1) was calculated from Garcia and Gordon (1992) as a function of salinity (here 0 ppt) and surface water temperature measured with the fast-responding dual O₂-temperature sensor ~54 cm below the air-water interface and then corrected for actual atmospheric pressure using Henry's law (average sea-level pressure of 1013.25 mbar corrected for elevation). The water column O₂ bulk concentration (C_{water} in Eq. 1) was measured with the same sensor. By substituting $J_{air-water}$ (Eq. 1) with the 15-min values for $J_{eddy, air-water}$ (Eq. 270 3), a gas exchange rate coefficient for O₂ was calculated from Eq. 1 and converted to the standard exchange coefficient, k_{600} , for CO₂ at 20 °C (Cole et al. 2010). For presentation, the 15-min k_{600} values were lumped in groups of four to give hourly values.

3 Results

275 All four deployments resulted in high-quality time series of the velocity field, the O₂
concentration, and the temperature ~54 cm below the air-water interface, and derived from
those, air-water fluxes of O₂ and heat, and gas exchange coefficients. These data and their
interpretation are presented below.

280 3.1 Data example

For a 40 h long deployment initiated on January 18, 2017 in the Moormans River, the 15-min
mean current velocity (Fig. 2a) was relatively constant, averaging 20.5 cm s⁻¹. The O₂
concentration measured with the fast-responding dual O₂-temperature sensor (Fig. 2b) agreed
closely with the concentration recorded with the independent sensor and showed a distinct
285 diurnal pattern. During most of the first night of the deployment, the O₂ concentration increased
linearly (h 19 to h 32), whereas a smaller and non-linear increase that tapered off was measured
during the second night (h 45 to h 56). A diurnal pattern was also seen in the calculated O₂
saturation concentration (Fig. 2b) reflecting variation in water temperature. The cumulative O₂
flux (Fig. 2c), with each data segment covering a 15-min time interval, had clear linear trends
290 indicating a strong eddy flux signal in the data. The hourly O₂ flux (Fig. 2d), representing means of
four successive 15-min flux estimates, also exhibited a clear diurnal pattern with a nighttime
average uptake by the river of 16.4 mmol m⁻² d⁻¹ for the first night, 9.1 mmol m⁻² d⁻¹ for the second
night, and an average daytime release of 11.1 mmol m⁻² d⁻¹. As observed for the O₂ concentration
(Fig. 2b), the hourly O₂ flux differed during the two nighttime periods with a close-to constant flux
295 during the first night and a flux that tapered off during the second night. The hourly standard gas
exchange coefficient (k_{600} , Fig. 2e) derived from the ~~hourly 15-min~~ O₂ flux (Fig. 2d) and the O₂
concentration difference over the air-water interface (Fig. 2b) was almost constant over the first
night of the deployment with an average of 3.9 m d⁻¹. After that, k_{600} diminished almost 3-fold to a
value of 1.4 m d⁻¹ during the daytime. During the second night, k_{600} tapered off markedly from a
300 level found for the first night to almost 0.89 m d⁻¹ during the last four h of the deployment. This
pattern was unexpected given the almost constant mean current velocity and insignificant winds
(Fig. 2a) and the similar O₂ concentration difference (Fig. 2b) for the two nighttime periods. The

pattern suggests that gas exchange was controlled by ~~a more dominant driver than the~~ at least one driver apart from the river current velocity or winds (see Discussion below).

The parallel results derived from the temperature data measured with the fast-responding dual O₂-temperature sensor agreed perfectly with the temperature recorded with the ~~stable~~ independent sensor (Fig. 3b) and had, as with the O₂ concentration, a distinct diurnal pattern. A close-to linear decrease occurred during the first night (h 18 to h 32) whereas a smaller and non-linear decrease that tapered off was recorded during the second night (h 45 to h 56). During the daytime the temperature increased. Unfortunately, we do not have reliable on-site measurements of the air temperature, but we infer that it, together with shortwave (sunlight during day) and longwave (nighttime) thermal radiation, controlled the recorded water temperature variations (Fig. 3b). The cumulative heat flux (Fig. 3c) had, as for O₂, clear linear trends indicating a strong flux signal in the data. The hourly heat flux (Fig. 3d) also exhibited a clear diurnal pattern with a nighttime average release of heat of 60.6 W m⁻² for the first night and 27.5 W m⁻² for the second night. As was observed for the temperature (Fig. 3b), the hourly heat flux showed different trends for the two nights with a close-to constant flux during the first night and a flux that tapered off during the second night.

Ignoring differences in the sign, representative cumulative co-spectra for the O₂ and heat fluxes (Fig. 4) during the first night (Figs. 2, 3) were similar in the 0.1 to 1 Hz frequency band with all substantial flux contributions for both the O₂ and heat fluxes having frequencies lower than ~0.9 Hz. ~~This result, combined with the fast-responding dual O₂-temperature sensor's response times ($t_{90\%}$) of 0.51 s for O₂ and 0.34 s for temperature (Berg et al. 2016), indicates that the entire eddy flux signal over all frequencies was accounted for in our measurements.~~

Due to careful leveling of the platform prior to data collection (Fig. 1b), rotation of the velocity field to correct for sensor tilt was minimal with an average of only 1.3° from horizontal. This rotation had an insignificant effect on the flux calculation. The applied time shift averaged 1.3 and

1.2 s for the O₂ and heat flux calculations, respectively, whereas the average storage correction (Eq. 3) amounted to 11 % for the O₂ flux and 15 % for the heat flux.

3.2 Representative gas exchange coefficients

335 The three other test deployments were shorter than the one presented in Figs. 2 and 3 but results were of comparable quality. Average values for selected parameters covering periods of time with several successive 15-min time intervals from all four deployments are given in Table 1. These periods were identified by containing consecutive time intervals with consistent standard gas exchange coefficient values, k_{600} , that had little variation and appeared to represent a particular
340 field condition. The longest period ($n = 51$) covers the first full night of the deployment shown in Fig. 2 (h 19 to h 32). Overall, the average current velocity varied from 8.3 to 28.4 cm s⁻¹ while k_{600} ranged from 0.4 to 5.1 m d⁻¹, or more than a factor of 12.

345 There was no significant relationship ($r = 0.37$, $p = 0.22$) between river current velocity and k_{600} values (Fig. 5) for all of the data in Table 1. Substantial variations in k_{600} values were found for some individual deployments even though the current velocity did not change markedly. Most prominently in the Moormans River deployment (Figs. 2, 3), where the k_{600} values varied more than a factor of 5. As we discuss below, this suggest that, at least for some sites and under some field conditions, other drivers of air-water gas exchange than river flow and winds are more
350 important.

3.3 Temperature effects on O₂ readings - a possible methodological bias

In the benthic environment the vertical turbulent heat flux is usually small relative to the O₂ flux due to slowly and modestly varying mean temperatures in the bottom water. At the air-water interface, however, the heat flux is typically larger due to substantial variations in air temperature and short- and long-wave thermal radiation, and the associated turbulent heat fluctuations can represent a challenge in O₂ flux measurements by eddy covariance.

360 ~~Highly~~All highly sensitive fast-responding O₂ sensors that can be used for aquatic eddy covariance measurements are to the best of our knowledge inherently sensitive to temperature ~~variations~~changes, and thus ~~they will~~ give variable O₂ readings at the same molar O₂ concentration if the temperature ~~changes~~varies. Typical temperature coefficients (% change in O₂ concentration reading caused by a temperature change of 1 °C) for Clark-type microelectrodes, still the most common sensor type used for aquatic eddy covariance, have values of ~3 % (Gundersen et al. 1998). Lab measurements in which the O₂ concentration was held constant but temperature varied showed that the fast-responding dual O₂-temperature sensor used in this study has a temperature coefficient of 2.9 % if temperature correction was omitted. This characteristic of fast-responding O₂ sensors implies that rapid temperature fluctuations associated with a turbulent heat flux will mistakenly be recorded as fluctuations in O₂ concentration and bias the eddy flux calculation unless an instantaneous temperature correction of the O₂ reading-signal is performed. In this study, this correction was done using the we relied on a new fast-responding dual O₂-temperature sensor's (Berg et al. 2016) which puts out rapid simultaneous readings of both the O₂-concentration and the temperature reading from within a distance of a few mm of the O₂ sensing foil and makes this correction possible. This was done for all O₂-fluxes we present. Below, we exemplify the nature and magnitude of this potential bias if this correction is omitted using data measured during the first night (h 18 to h 32) of the deployment ~~depicted~~shown in Figs. 2 and 3.

380 The turbulent temperature fluctuations for a 3-min period shown in Fig. 6a are associated with a vertical heat flux of ~60 W m⁻² (Fig. 3d) and amount to ± ~0.015 °C. Based on a temperature coefficient of ~3 %, according to the O₂-calibration equation provided by the producer of our sensor (JFE Advantech, Japan), this translates into fluctuations in O₂ concentration readings of ± ~0.2 μmol L⁻¹ (Fig. 6a, right axis). Using such 'simulated' O₂ data, derived from the 8 Hz nighttime temperature data (Fig. 3, h 18 to h 32), representing solely temperature sensitivity effects and no true O₂ reading, and produced from the 8 Hz nighttime temperature data (h 18 to h 32, Fig. 3), to calculate produced an O₂ release, or flux bias, gives a release of 11.9 mmol m⁻² d⁻¹ (blue bar, Fig.

6b). Using the instantaneous temperature corrected O₂ data, as was done for all other calculations we present, gives an oppositely directed O₂ uptake of 16.9 mmol m⁻² d⁻¹ (red bar, Fig. 6b). ~~whereas using~~ Using the sensor's O₂ readings, but without the ~~rapid~~ instantaneous temperature correction, gives a release of only 4.4 mmol m⁻² d⁻¹ (green bar, Fig. 6b).

The magnitude of this O₂ flux bias if temperature correction is omitted, scales with the heat flux and is proportional with the O₂ sensor's temperature coefficient and the actual O₂ concentration. Given the mm-close proximity of the temperature thermistor and the O₂ sensing foil and the relatively small difference between the fast-responding dual O₂-temperature sensor's response times (0.51 for O₂ and 0.34 s for temperature, Berg et al., 2016), we conclude that the effects of temperature sensitivity were removed from our O₂ flux calculations. This point is supported by the high-frequency end (~0.9 Hz) of the co-spectra for the O₂ and heat fluxes (Fig. 4).

4 Discussion

Deploying the aquatic eddy covariance technique right below the air-water interface provided a feasible way to determine gas exchange rates and coefficients. Relative to what is possible with traditional methods, this new approach gives gas exchange rates and coefficients with an improved precision and at a higher spatial and temporal resolution. For those reasons, the approach has the potential to enhance our knowledge ~~on~~ of the dynamics and controls of gas exchange and thus benefit aquatic ecosystem studies and pave the way for new lines of ecosystem research.

These points are exemplified in our longest test deployment that lasted 40 h (Figs. 2, 3) and resulted in aquatic eddy covariance data for both O₂ and temperature of a quality and internal consistency that fully match those published for many benthic environments (see review by Berg et al. (2017)). Specifically, the 8 Hz velocity, O₂, and temperature data (Figs. 2a, 2b, 3b) were recorded with low noise and the O₂ and temperature data perfectly matched measurements with the stable independent sensor (Figs. 2b, 3b). Furthermore, the cumulative fluxes (Figs. 2c, 3c) had

415 clear linear trends that indicate a strong and consistent flux signal in the data, and the times
where the hourly O₂ flux changed direction (Fig. 2d, positive values represent a release), matched
exactly the times ~~where~~ when the driving O₂ ~~concentration~~ concentration difference changed sign
(Fig. 2b). Moreover, the cumulative co-spectra for the O₂ and ~~the temperature~~ heat fluxes (Fig. 4)
have the shape typically seen for shallow-water environments (Lorrai et al. 2010; Berg et al.
420 2013). The fact that all flux contributions for both the O₂ and heat fluxes had frequencies lower
than ~0.9 Hz, combined with the fast-responding dual O₂-temperature sensor's response times
($t_{90\%}$) of 0.51 s for O₂ and 0.34 s for temperature (Berg et al. 2016), indicates that the entire flux
signal over all frequencies was captured. Finally, for both O₂ and temperature there was a clear
relationship between the flux over the air-water interface (Figs. 2d, 3d) and the observed change
425 in the water column (Figs. 2b, 3b). For O₂, for example, the ratio between the averaged fluxes for
the two nights (Fig. 2d, h 21 to h 30 vs. h 45 to h 54, Fig. 2d) equals 2.0 which is close to the ratio
of 2.2 between the changes in water column concentrations (Fig. 2b) for the same two periods.

Both the O₂ and ~~the~~ temperature data (Figs. 2b, 2d, 3b, 3d) contained a clear diurnal signal overall.
430 For O₂, however, this was not driven by biological processes, i.e. net primary O₂ production during
daytime and respiration during nighttime, as this would have resulted in an increase in mean
water column O₂ concentration during daytime and a decrease at nighttime. That the opposite
pattern was found indicates that physical processes related to thermal conditions were
controlling the O₂ dynamics. Specifically, colder nighttime air temperatures and possibly also
435 long-wave thermal radiation to the atmosphere were driving the substantial heat flux out of the
river (Fig. 3d) which resulted in ~~the~~ falling water temperatures (Fig. 3b). This, in turn, was
changing changed the O₂ saturation concentration (C_{air} in Eq. 1) and thus the driving
concentration difference of O₂ exchange over the air-water interface (Fig. 2b). During the daytime,
the reverse pattern was in place. This rather complex relationship, or linkage via physical
440 processes, is the only mechanism that can explain the overall pattern found for this deployment
(Figs. 2, 3). Considering that these measurements were done under conditions that did not
include any uncommon or extreme weather conditions suggests that physical processes, and not

biological processes, are often an important, or even the main, driver of O₂ dynamics in shallow-water rivers and streams. An unfortunate consequence of this dominance or control by physical conditions, which we believe is not yet fully recognized, is that it adds substantial uncertainty to the widely used approach of deriving metabolic estimates (e.g., gross primary production, respiration, net ecosystem metabolism) from time series of measured water column O₂ concentrations (Odum 1956; Hall et al. 2016).

The standard gas exchange coefficients (k_{600}) for all of our four deployments (distributed on three different river sites, all with smooth quietly flowing water without standing riffles or waves, Fig.1) did not show a significant relationship with river current velocity (Fig. 5, Table 1). This is in line with previously published results from across-site comparisons (Hall et al. 2016), but the substantial variation among k_{600} values for some individual deployments (in particular for the Moormans River deployment, Figs. 2d) despite only moderately varying river flow velocity and insignificant winds is surprising. For example, k_{600} varied from a close-to constant value of 3.9 m d⁻¹ during the first night (Fig. 2e, h 19 to h 32, Fig. 2e), followed by an almost 3 times smaller daytime value of 1.4 m d⁻¹ (h 33 to h 42), and then increased again at the onset of the second night before finally tapering off to a small value of 0.9 m d⁻¹ (h 52 to h 56) at the end of the deployment. The co-variance of the heat exchange (Fig. 3d) suggests that turbulence, or turbulent-like motions (which stimulates gas exchange) was generated by natural convective forces driven by the substantial heat-loss from the river during the nighttime (Fig. 3d). Conversely, during the daytime, when the heat flux was directed into the river (Fig. 3d), turbulent motions were presumably dampened by vertical temperature stratifications in the surface water. Given the 'low-energy' smooth and quietly flowing water, we find this explanation for the varying k_{600} values (Fig. 2e) likely and note that ~~it~~ this controlling factor has been described before (Bannerjee and MacIntyre 2004; MacIntyre et al. 2010). We also note that this observed complex pattern illustrates the difficulties that can be associated with determining accurate air-water gas exchange rates and coefficients without direct site- and time-specific measurements.

An important methodological finding linked to the new approach is that O₂ sensor readings should, at least in some cases, be corrected for temperature sensitivity using concurrent rapid high-speed temperature readings as was done here for all O₂ fluxes used to estimate air-water gas exchange coefficients (Fig. 2, Table 1). In the benthic environment ~~where the aquatic eddy covariance technique for O₂ flux measurements was first developed (Berg et al. 2003)~~, the vertical turbulent heat flux is usually small relative to the O₂ flux due to slowly and modestly varying mean temperatures in the bottom water. ~~At the air-water interface, however, the heat flux is typically larger due to substantial variations in air temperatures and short- and long-wave thermal radiation. As a result,~~ However, results presented here show that rapid temperature fluctuations associated with the substantial turbulent heat flux below the air-water interface ~~will~~can mistakenly be recorded as fluctuations in the O₂ concentration ~~if this correction is omitted~~ and bias the O₂ flux calculation ~~substantially significantly if instantaneous temperature correction is omitted~~ (Fig. 6). It is unclear how widespread this problem is – more studies are needed to determine that – but in the example included here, this bias alters the flux by more than a factor of 2-3 (Fig. 6). Our data were recorded during winter, and one could argue that the O₂ exchange would be much larger during summer due to extensive primary production and respiration which would reduce the relative magnitude of this bias (Fig. 6). But as the O₂ flux is indeed likely to be more pronounced during summer than during winter, so is the heat flux.

5 Summary and recommendations

Based on our proof-of-concept deployments, the aquatic eddy covariance technique applied right below the air-water interface should be particularly useful in detailed studies of gas exchange that evaluate its dynamics and controls. The approach can consequently help reduce the generally recognized problem of large uncertainties linked to gas exchange estimates in traditional aquatic ecosystem studies.

The floating platform we used here for measuring aquatic eddy covariance fluxes right below the air-water interface (Fig. 1) can easily be reproduced as it relies exclusively on standard materials

and commercially available instrumentation, the latter designed with plug-and-play capabilities.

500 Furthermore, standard software for eddy flux extractions developed for the benthic environment or for the atmospheric boundary layer can be used to estimate air-water fluxes.

We recommend that eddy covariance data are recorded close to the air-water interface (Fig. 1c) to minimize the effects of the O₂ storage in the water between the measuring point and the surface and because gradients of both O₂ and temperature can form in the upper water column. We also
505 recommend that simultaneous rapid-high-speed temperature measurements are performed within a few mm of the O₂ concentration recordings to allow for instantaneous temperature corrections of the O₂ signal (Fig. 6).

510 Finally, our results illustrate that the O₂ concentration difference driving the air-water gas exchange is often small (Fig. 2), here < 2 % of the absolute concentration. This emphasizes the importance of relying both on accurately calibrated sensors to measure the water bulk concentration (C_{water} in Eq. 1) and precise determinations of the saturation concentration (C_{air} in Eq. 1) that is corrected for temperature, salinity, and atmospheric pressure.

515

6 Future work

A further development of the new application of the aquatic eddy covariance technique presented here is to perform similar measurements from a moving platform in small lakes, reservoirs, and estuaries. In these environments, gas exchange and gas exchange coefficients are expected to vary
520 spatially, for example from the lee to windward side of the aquatic system. By using a floating autonomously moving platform, we anticipate that such variations can be spatially mapped out and studied. We are currently performing the first tests along these lines.

7 Acknowledgements

525 This study was supported by grants from the National Science Foundation (ESC-1550822, OCE-1334848) and the University of Virginia. We thank Julie and John Baird, Nancy and Ed Mcmurdo,

Martha Hodgkins, and Brian Richter who allowed us to work on their beautiful properties in the Hardware River, the Mechums River, and the Moormans River. Finally, we thank Rachel E. Michaels for editorial assistance on the manuscript.

530 8 References

- Anderson, D. E., R. G. Striegl, D. I. Stannard, C. M. Michmerhuizen, T. A. McConnaughey, and J. W. LaBaugh. 1999. Estimating lake-atmosphere CO₂ exchange. *Limnol. Oceanogr.* **44**: 988-1001.
- 535 Bannerjee, S., and S. MacIntyre. 2004. The air–water interface: turbulence and scalar interchange. *Advances in coastal and ocean engineering* **9**: 181-237.
- Bastviken, D., L. J. Tranvik, J. A. Downing, P. M. Crill, and A. Enrich-Prast. 2011. Freshwater Methane Emissions Offset the Continental Carbon Sink. *Science* **331**: 50-50.
- Berg, P., M. L. Delgard, R. N. Glud, M. Huettel, C. E. Reimers, and M. L. Pace. 2017. Non-invasive Flux Measurements at the Benthic Interface: the Aquatic Eddy Covariance Technique. *Limnol. Oceanogr.:* e-Lectures **doi: 10.1002/loe2.10005**.
- 540 Berg, P., D. Koopmans, M. Huettel, H. Li, K. Mori, and A. Wüest. 2016. A new robust dual oxygen-temperature sensor for aquatic eddy covariance measurements. *Limnol. Oceanogr.:* Methods **14**: 151–167.
- Berg, P., M. H. Long, M. Huettel, J. E. Rheuban, K. J. McGlathery, R. W. Howarth, K. H. Foreman, A. E. Giblin, and R. Marino. 2013. Eddy correlation measurements of oxygen fluxes in permeable sediments exposed to varying current flow and light. *Limnol. Oceanogr.* **58**: 1329–1343.
- 545 Berg, P., H. Roy, F. Janssen, V. Meyer, B. B. Jorgensen, M. Huettel, and D. de Beer. 2003. Oxygen uptake by aquatic sediments measured with a novel non-invasive eddy-correlation technique. *Marine Ecology Progress Series* **261**: 75-83.
- 550 Billett, M., and T. Moore. 2008. Supersaturation and evasion of CO₂ and CH₄ in surface waters at Mer Bleue peatland, Canada. *Hydrological Processes* **22**: 2044-2054.
- Borges, A. V., B. Delille, L. S. Schiettecatte, F. Gazeau, G. Abril, and M. Frankignoulle. 2004. Gas transfer velocities of CO₂ in three European estuaries (Randers Fjord, Scheldt, and Thames). *Limnol. Oceanogr.* **49**: 1630-1641.
- 555 Butman, D., and P. A. Raymond. 2011. Significant efflux of carbon dioxide from streams and rivers in the United States. *Nature Geoscience* **4**: 839-842.
- Cole, J. J., D. L. Bade, D. Bastviken, M. L. Pace, and M. Van de Bogert. 2010. Multiple approaches to estimating air-water gas exchange in small lakes. *Limnology And Oceanography-Methods* **8**: 285-293.
- 560 Cole, J. J., Y. T. Prairie, N. F. Caraco, W. H. McDowell, L. J. Tranvik, R. G. Striegl, C. M. Duarte, P. Kortelainen, J. A. Downing, J. J. Middelburg, and J. Melack. 2007. Plumbing the global carbon cycle: Integrating inland waters into the terrestrial carbon budget. *Ecosystems* **10**: 171-184.
- Fritzsche, E., P. Gruber, S. Schutting, J. P. Fischer, M. Strobl, J. D. Müller, S. M. Borisov, and I. Klimant. 2017. Highly sensitive poisoning-resistant optical carbon dioxide sensors for environmental monitoring. *Analytical Methods* **9**: 55-65.
- 565 Garcia, H. E., and L. I. Gordon. 1992. Oxygen solubility in seawater: Better fitting equations. *Limnol. Oceanogr.* **37**: 1307-1312.
- Genereux, D. P., and H. F. Hemond. 1992. Determination of gas exchange rate constants for a small stream on Walker Branch Watershed, Tennessee. *Water Resources Research* **28**: 2365-2374.

- 570 Gundersen, J. K., N. B. Ramsing, and R. N. Glud. 1998. Predicting the signal of O-2 microsensors from physical dimensions, temperature, salinity, and O-2 concentration. *Limnology & Oceanography* **43**: 1932-1937.
- Hall, R. O., J. L. Tank, M. A. Baker, E. J. Rosi-Marshall, and E. R. Hotchkiss. 2016. Metabolism, gas exchange, and carbon spiraling in rivers. *Ecosystems* **19**: 73-86.
- 575 Hanson, P. C., A. I. Pollard, D. L. Bade, K. Predick, S. R. Carpenter, and J. A. Foley. 2004. A model of carbon evasion and sedimentation in temperate lakes. *Global Change Biology* **10**: 1285-1298.
- Holst, G., R. N. Glud, M. Kuhl, and I. Klimant. 1997. A Microoptode Array For Fine-Scale Measurement of Oxygen Distribution. *Sensors & Actuators B Chemical* **38**: 122-129.
- Holst, G., O. Kohls, I. Klimant, B. Konig, M. Kuhl, and T. Richter. 1998. A modular luminescence lifetime imaging system for mapping oxygen distribution in biological samples. *Sensors and*
580 *Actuators B-Chemical* **51**: 163-170.
- Hume, A. C., P. Berg, and K. J. McGlathery. 2011. Dissolved oxygen fluxes and ecosystem metabolism in an eelgrass (*Zostera marina*) meadow measured with the eddy correlation technique. *Limnol. Oceanogr.* **56**: 86-96.
- 585 Jonsson, A., J. Åberg, A. Lindroth, and M. Jansson. 2008. Gas transfer rate and CO₂ flux between an unproductive lake and the atmosphere in northern Sweden. *Journal of Geophysical Research: Biogeosciences* **113**.
- Klimant, I., V. Meyer, and M. Kuehl. 1995. Fiber-optic oxygen microsensors, a new tool in aquatic biology. *Limnol. Oceanogr.* **40**: 1159-1165.
- 590 Koopmans, D. J., and P. Berg. 2015. Stream oxygen flux and metabolism determined with the open water and aquatic eddy covariance techniques. *Limnol. Oceanogr.* **60**: 1344-1355.
- Liss, P., and P. Slater. 1974. Flux of gases across the air-sea interface. *Nature* **247**: 181-184.
- Long, M. H., P. Berg, D. de Beer, and J. C. Zieman. 2013. In situ coral reef oxygen metabolism: An eddy correlation study. *Plos One* **8**: e58581. doi:58510.51371/journal.pone.0058581.
- 595 Lorke, A., D. F. McGinnis, A. Maeck, and H. Fischer. 2012. Effect of ship locking on sediment oxygen uptake in impounded rivers. *Water Resources Research* **48**.
- Lorrai, C., D. F. McGinnis, P. Berg, A. Brand, and A. Wüest. 2010. Application of oxygen eddy correlation in aquatic systems. *Journal of Atmospheric and Oceanic Technology* **27**: 1533-1546.
- MacIntyre, S., A. Jonsson, M. Jansson, J. Aberg, D. E. Turney, and S. D. Miller. 2010. Buoyancy flux, turbulence, and the gas transfer coefficient in a stratified lake. *Geophysical Research Letters* **37**.
- 600 Macintyre, S., R. Wanninkhof, and J. P. Chanton. 1995. Trace gas exchange across the air-water interface in freshwater and coastal marine environments, p. 52-97. *In* R. C. H. P.A. Matson [ed.], *Biogenic Trace Gases: Measuring Emissions from Soil and Water*. Blackwell Science Ltd.
- Mammarella, I., A. Nordbo, Ü. Rannik, S. Haapanala, J. Levula, H. Laakso, A. Ojala, O. Peltola, J. Heiskanen, J. Pumpanen, and T. Vesala. 2015. Carbon dioxide and energy fluxes over a small boreal lake in Southern Finland. *Journal of Geophysical Research: Biogeosciences*:
605 2014JG002873.
- Marino, R., and R. W. Howarth. 1993. Atmospheric oxygen-exchange in the Hudson River - Dome measurements and comparison with other natural-waters. *Estuaries* **16**: 433-445.
- 610 McKenna, S., and W. McGillis. 2004. The role of free-surface turbulence and surfactants in air-water gas transfer. *International Journal of Heat and Mass Transfer* **47**: 539-553.

- Odum, H. T. 1956. Primary production in flowing waters. *Limnol. Oceanogr.* **1**: 103-117.
- Raymond, P., and J. Cole. 2001. Gas exchange in rivers and estuaries: Choosing a gas transfer velocity. *Estuaries* **24**: 312-317.
- 615 Raymond, P. A., J. Hartmann, R. Lauerwald, S. Sobek, C. McDonald, M. Hoover, D. Butman, R. Striegl, E. Mayorga, C. Humborg, P. Kortelainen, H. Durr, M. Meybeck, P. Ciais, and P. Guth. 2013. Global carbon dioxide emissions from inland waters. *Nature* **503**: 355-359.
- Raymond, P. A., C. J. Zappa, D. Butman, T. L. Bott, J. Potter, P. Mulholland, A. E. Laursen, W. H. McDowell, and N. D. 2012. Scaling the gas transfer velocity and hydraulic geometry in streams and small rivers. *Limnology and Oceanography: Fluids & Environments* **2**: 41-53.
- 620 Rheuban, J. E., P. Berg, and K. J. McGlathery. 2014. Multiple timescale processes drive ecosystem metabolism in eelgrass (*Zostera marina*) meadows. *Marine Ecology Progress Series* **507**: 1-13.
- Rovelli, L., K. M. Attard, L. D. Bryant, S. Flögel, H. J. Stahl, M. Roberts, P. Linke, and R. N. Glud. 2015. Benthic O₂ uptake of two cold-water coral communities estimated with the non-invasive eddy-correlation technique. *Marine Ecology Progress Series* **525**: 97-104.
- 625 Van de Bogert, M. C., D. L. Bade, S. R. Carpenter, J. J. Cole, M. L. Pace, P. C. Hanson, and O. C. Langman. 2012. Spatial heterogeneity affects estimates of ecosystem metabolism in two northern lakes. *Limnol. Oceanogr.* **57**: 1689-1700.
- Van de Bogert, M. C., S. R. Carpenter, J. J. Cole, and M. L. Pace. 2007. Assessing pelagic and benthic metabolism using free water measurements. *Limnology And Oceanography-Methods* **5**: 145-155.
- 630 Wanninkhof, R. 1985. Kinetic fractionation of the carbon isotopes ¹³C and ¹²C during transfer of CO₂ from air to seawater. *Tellus B* **37**: 128-135.
- Wanninkhof, R., P. J. Mulholland, and J. W. Elwood. 1990. Gas-exchange rates for a 1st-order stream determined with deliberate and natural tracers. *Water Resources Research* **26**: 1621-1630.
- 635 Watson, A. J., R. C. Upstill-Goddard, and P. S. Liss. 1991. Air-sea gas exchange in rough and stormy seas measured by a dual-tracer technique. *Nature* **349**: 145-147.
- Whitman, W. G. 1923. The two film theory of gas absorption. *Chemical and Metallurgical Engineering* **29**: 146-148.
- 640

9 Tables

Deployment -	Start date -	<i>n</i> -	Current velocity cm s ⁻¹	O ₂ flux mmol m ⁻² d ⁻¹	<i>k</i> ₆₀₀ m d ⁻¹
Hardware River, dep. 1	Nov 22, 2015	20	28.4	9.1	1.6
"	"	39	27.5	12.0	2.7
"	"	13	27.6	-10.7	2.5
Hardware River, dep. 2	Sep 14, 2016	20	8.7	7.0	0.4
"	"	4	8.3	9.4	0.7
Mechums River	Dec 21, 2016	23	9.4	-42.9	2.3
"	"	36	9.3	-29.2	1.7
Moormans River	Jan 18, 2017	4	25.6	-8.9	1.9
"	"	51	18.4	16.8	3.9
"	"	34	20.4	-11.8	1.3
"	"	3	22.9	19.3	5.1
"	"	16	23.4	10.1	2.1
"	"	26	21.3	5.8	1.0

Table 1: Representative standard gas exchange coefficients (k_{600}) along with current velocity and O₂ flux for four deployments at three different sites. The third column (n) specifies the number of 15-min time intervals included in the averages. Values from the last deployment (Moormans River) are depicted in Figs. 2 and 3.

10 Figures



Figure 1: Floating platform for determining air-water gas exchange. **(a)** The 120 cm long and 90 cm 1.2×0.9 m wide platform with a catamaran-shaped hull being prepared for deployment. Four inflatable fenders provide flotation. **(b)** The platform deployed in the Hardware River and anchored to both river banks. A dive weight is used to level the platform. **(c)** Close-up look at: 1) the three-pronged upward-facing sensor head of the cabled Acoustic Doppler Velocimeter (cabled Vector, Nortek AS, Norway), 2) the fast-responding dual O₂-temperature sensor (RINKO EC, JFE Advantech, Japan), and 3) Two stable independent dual O₂-temperature sensors used for calibration (miniDOT, PME, USA).

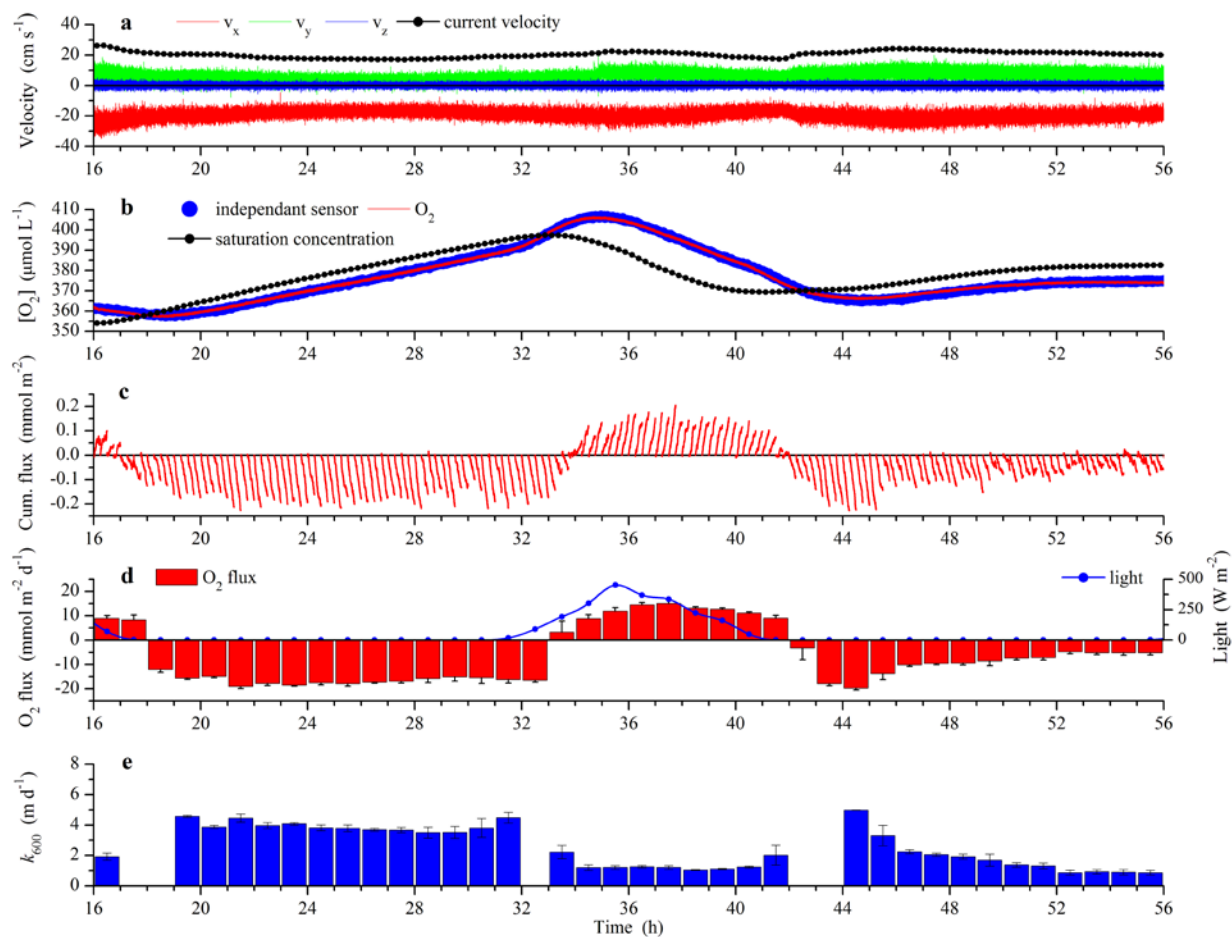


Figure 2: Forty h long test deployment initiated at 16:00 in the afternoon as indicated on the x-axis. **(a)** Three velocity components at 8 Hz (x, y, z ; z is vertical) and 15-min mean current velocity. **(b)** O₂ concentration at 8 Hz measured with the dual O₂-temperature sensor and at 1-min measured with an independent sensor. **(c)** Cumulative flux over 15-min time intervals with clear linear trends. **(d)** Hourly O₂ flux (positive values represent a release from the river), each value based on 15-min flux extractions ($n = 4$, SE) and day light measured at a nearby weather station. **(e)** Hourly standard gas exchange coefficient (k_{600}) based on 15-min estimates ($n = 4$, SE). The few gaps in the data are for the times where the driving O₂ concentration difference changes sign (panel c).

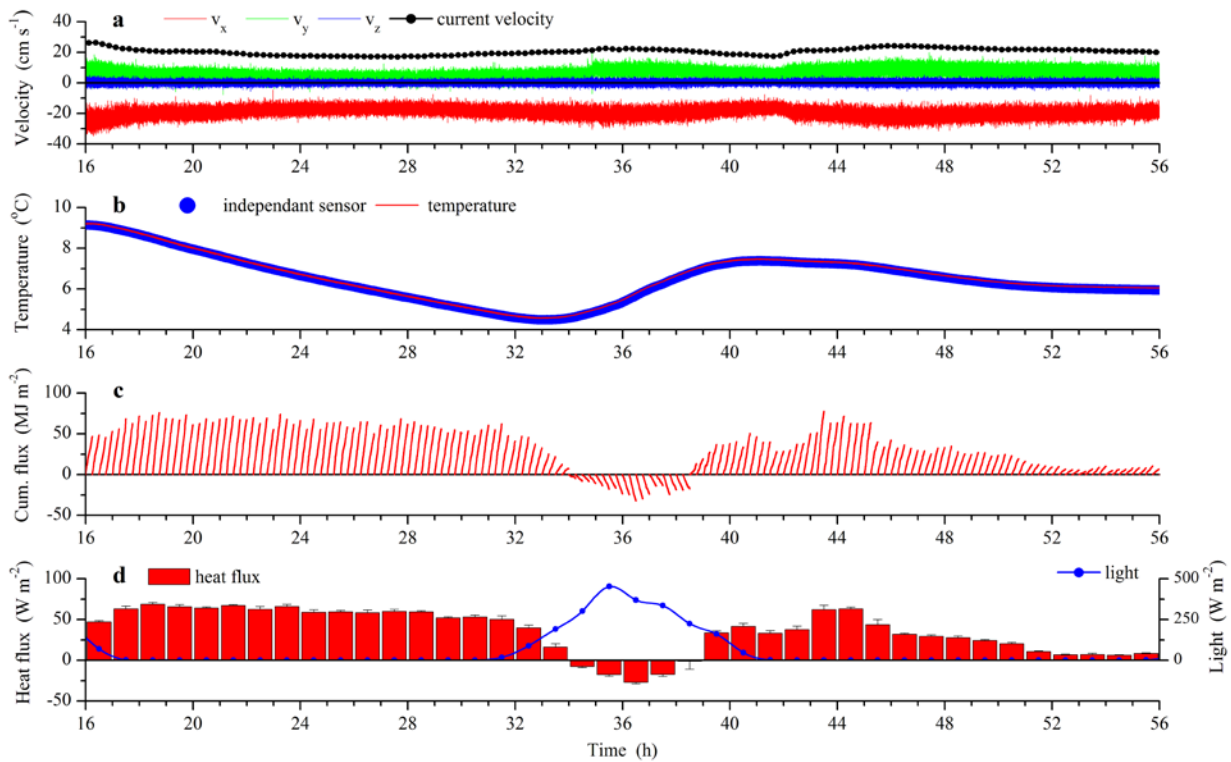


Figure 3: Same-The same deployment as in Fig. 2, but with results for temperature and heat. The deployment was initiated at 16:00 in the afternoon as indicated on the x-axis. **(a)** Three velocity components at 8 Hz (x, y, z ; z is vertical) and 15-min mean current velocity. **(b)** Temperature at 8 Hz measured with the dual O₂-temperature sensor and at 1-min measured with an independent optode. **(c)** Cumulative flux over 15-min time intervals with clear linear trends. **(d)** Hourly heat flux, each value based on 15-min flux extractions ($n = 4$, SE) and day light measured at a nearby weather station. Positive flux values represent a release of heat from the river.

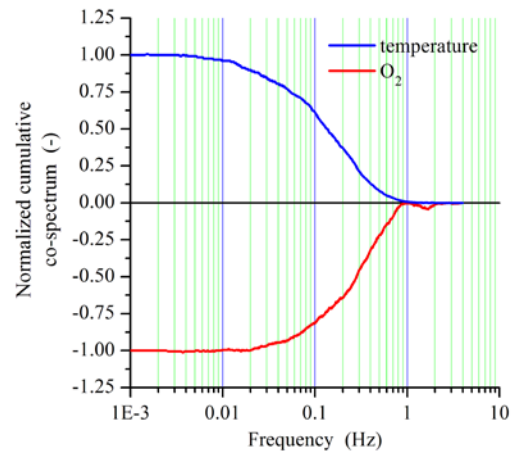


Figure 4: Nighttime normalized cumulative co-spectra for the vertical velocity combined with the O₂ concentration and the temperature, respectively, revealing which frequencies carried the eddy flux signal.

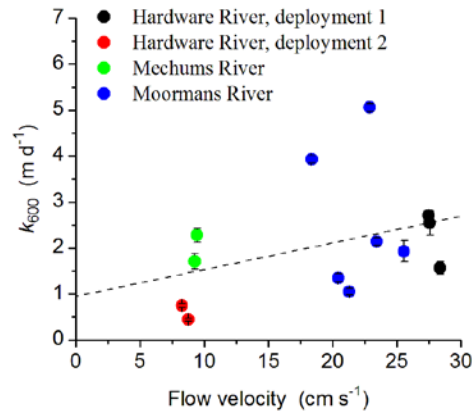


Figure 5: Standard gas exchange coefficient, k_{600} , plotted against river current velocity. The dotted line is a linear fit to all data ($R = 0.37$, $p = 0.22$).

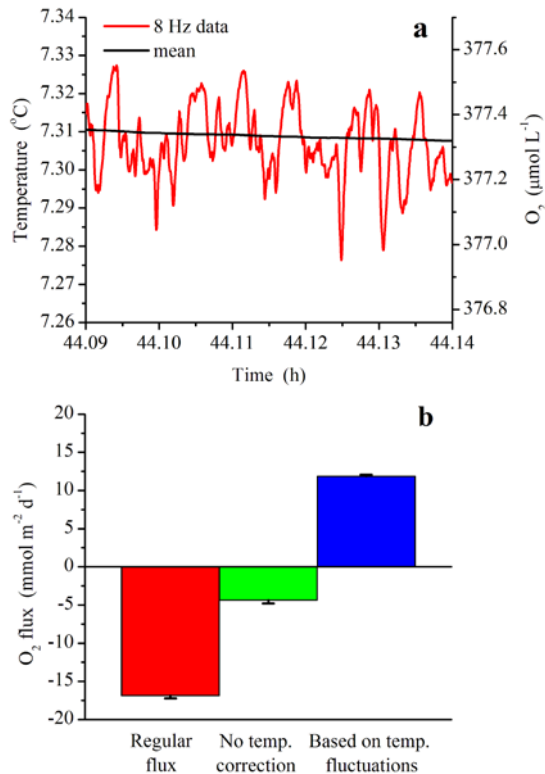


Figure 6: Bias that can arise if O₂ concentration sensor readings are not corrected using rapid parallel temperature measurements. **(a)** Recorded 8 Hz data of temperature fluctuations and their mean (left axis) through 3-min and the resulting fluctuations in O₂ concentration that would be recorded solely due to temperature sensitivity by a sensor with a temperature coefficient of 3 % (right axis). **(b)** Average air-water fluxes, all for the same period of the first night (h 18 to h 32) of the deployment depicted in Figs. 2 and 3, calculated using instantaneous temperature corrected data (red bar), data without rapid temperature correction (green bar), and ‘simulated’ data produced from rapid-8Hz temperature recordings as shown in panel **a** and assuming a temperature coefficient of 3 % (blue bar).